

GLAD: Generalizable Tuning for Vision-Language Models

Yuqi Peng^{1,2} Pengfei Wang³ Jianzhuang Liu¹ Shifeng Chen^{1,4*}

¹Shenzhen Institutes of Advanced Technology, Chinese Academy of Sciences

²Northeastern University ³The Hong Kong Polytechnic University

⁴Shenzhen University of Advanced Technology

peng.yuq@northeastern.edu, pengfei.wang@connect.polyu.hk,
jz.liu@siat.ac.cn, shifeng.chen@siat.ac.cn

Abstract

*Pre-trained vision-language models, such as CLIP, show impressive zero-shot recognition ability and can be easily transferred to specific downstream tasks via prompt tuning, even with limited training data. However, existing prompt tuning methods face two main challenges: (1) In few-shot scenarios, data scarcity often leads to overfitting, making the model sensitive to changes in the input domain. (2) To mitigate overfitting, these methods typically rely on complex task-specific model architectures and sensitive hyperparameter tuning, severely restricting their general applicability. To address these issues, we propose a simpler and more general framework called **GLAD** (**G**eneralizable **L**oRA tuning with **R**egularized **G**radient). We show that merely applying LoRA achieves performance in downstream tasks comparable to current state-of-the-art prompt-based methods. While LoRA is effective and easy to use, it remains susceptible to overfitting in few-shot learning scenarios. To mitigate this risk, we introduce a gradient-based regularization technique. This technique effectively steers the optimization trajectory, encouraging the model to find a more stable parameter region that is robust to variations in data distribution. Through extensive experiments conducted on 15 benchmark datasets, we demonstrate that GLAD outperforms previous tuning approaches in terms of base-to-novel class generalization, image domain generalization, and cross-dataset generalization. The code will be publicly available.*

1. Introduction

Foundational vision-language models have demonstrated remarkable capabilities across a variety of visual tasks, in-

cluding object detection [6, 8, 12, 65], image classification [40, 43, 58], segmentation [32], and image description generation [26, 34, 63]. Among these models, CLIP [40] has received significant attention due to its strong zero-shot recognition performance. CLIP employs contrastive learning on a large-scale dataset of image-text pairs sourced from the internet, mapping both visual and textual inputs into a shared embedding space. This approach endows CLIP with robust recognition capabilities in open-world settings, achieving strong performance even on rare data.

Although CLIP demonstrates outstanding performance across domains, adapting it to a specific downstream tasks under limited annotated data conditions remains a significant challenge [66]. Traditional full-parameter fine-tuning approaches often compromise the generalization capability acquired during pre-training, leading to catastrophic forgetting in few-shot setting. Prompt Tuning [20, 21, 24, 31, 55, 61, 66–68], as a more parameter-efficient adaptation method, achieves few-shot adaptation by appending a set of learnable vectors to the input embeddings while keeping the backbone model frozen. However, this approach relies on few task-specific samples for optimizing the learnable vectors, making it prone to overfitting [31, 61, 66, 67]. To address this, various methods [21, 24] have proposed different prompt insertion[66] schemes, model structures[20, 24], and objectives[21]. However, these often require task-specific architectures, complex regularization, or carefully tuned hyperparameters, limiting scalability to new tasks.

In this work, we propose GLAD, a simple yet effective fine-tuning framework designed to improve generalization in vision-language models. Unlike previous prompt tuning approaches [20, 21, 24, 31, 55, 66–68], GLAD leverages Low-Rank Adaptation (LoRA) [16], which inserts trainable low-rank matrices into each transformer layer while keeping the pretrained parameters frozen. Surprisingly, we find that even a naive application of LoRA without any specific design can achieve performance comparable to recent state-

*Corresponding author: Shifeng Chen. This work was supported by the Shenzhen Science and Technology Program (JSGG20220831105002004) and the Shenzhen Key Laboratory of Computer Vision and Pattern Recognition.

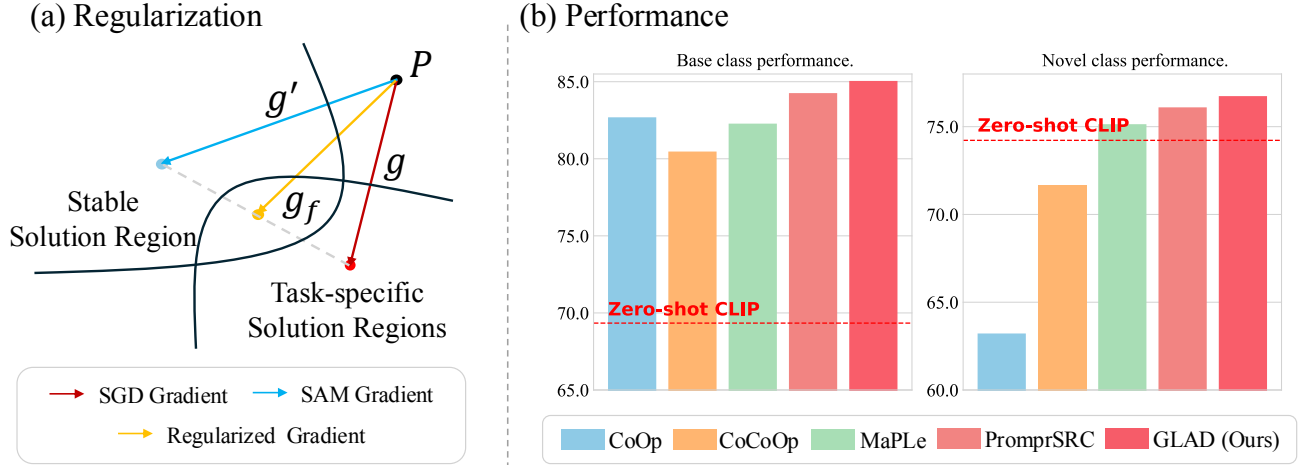


Figure 1. An overview of the proposed regularization strategy and its effect on base-to-novel generalization. (a) Illustration of our gradient regularization mechanism. We use the gradient computed via Sharpness-Aware Minimization (SAM) as a reference signal to steer the original gradient direction toward a region shared by both stable solutions and task-specific solutions. This regularization promotes convergence to parameter regions that are both robust and task-relevant. (b) Comparison of GLAD with existing prompt learning methods in terms of base (seen during training) and novel (unseen during training) class accuracy across 11 datasets. GLAD consistently outperforms prior methods on both categories, demonstrating stronger generalization in few-shot settings.

of-the-art prompt tuning methods on downstream classification tasks.

Nevertheless, LoRA alone still has limitations in few-shot settings, where the scarcity of labeled data often leads to overfitting and makes the model less flexible in handling distributional shifts, resulting in poor generalization. To address this, we propose two complementary enhancements: a lightweight AlignNet module and a gradient-based regularization strategy. AlignNet dynamically adjusts textual features by conditioning on both visual and textual representations, enabling more adaptive text embeddings that better align with varying image input distributions. This improves the model’s flexibility in encoding semantics and strengthens its ability to generalize to new downstream task domains. In parallel, as illustrated in Figure 1(a), our gradient regularization technique steers the optimization direction toward stable regions in the parameter space, where the model’s performance is more robust to variations in data distribution. This leads to improved robustness under distribution shifts and helps prevent overfitting in few-shot settings. Figure 1(b) further illustrates that our method consistently outperforms prior approaches in base-to-novel generalization.

Our contributions are summarized as follows:

- We present **GLAD**, the first framework dedicated to improving the generalization ability of **LoRA** in few-shot learning scenarios. Our design enables efficient and scalable adaptation to new images, categories, and task domains under few-shot supervision.
- We develop a novel **gradient-based regularization strategy** that steers the optimization direction toward flat-

ter regions in the loss landscape. By aligning gradients with worst-case gradient directions, the method stabilizes optimization and mitigates overfitting under data scarcity, ultimately improving robustness to distribution shifts.

- We conduct extensive classification experiments across three generalization settings: base-to-novel class generalization, image domain generalization, and cross-dataset generalization. GLAD consistently outperforms strong prompt tuning baselines and achieves state-of-the-art performance across all generalization tests, demonstrating its effectiveness in improving model performance and robustness under distributional shifts.

2. Related Work

In this section, we review three lines of related work that form the foundation of our method: prompt tuning in vision-language models, low-rank adaptation techniques for efficient fine-tuning, and regularization strategies for generalization.

2.1. Prompt Tuning for Vision-Language Models

Prompt tuning has emerged as a parameter-efficient fine-tuning strategy, originally developed in natural language processing to guide pre-trained models using learnable prompt vectors [25, 29]. In the context of VLMs, Zhou et al. [67] proposed CoOp, which replaces handcrafted textual templates (e.g., “a photo of a [CLASS]”) with continuous learnable embeddings prepended to class tokens. While CoOp has achieved impressive performance in few-shot classification, its prompts tend to overfit the seen data distribution, leading to poor generalization ability.

To address overfitting in prompt tuning, many works

introduce specialized designs. Some modify architectures to limit parameter updates and enhance flexibility, such as RPO [24], MaPLe [20], VPT [19], and DePT [61]. Others leverage prior knowledge from pre-trained models to guide learning, including PromptSRC [21], PromptKD [27], TCP [55], and Quaternion Prompt [2]. Additionally, methods like CoCoOp [66] and MM-Align [49] enhance cross-modal interactions to improve adaptation to distribution shifts.

In contrast, our approach eliminates the need for explicit prompt design by structurally modifying the model through LoRA. Additionally, we introduce a lightweight AlignNet that aligns the final text and visual features after encoding, enabling instance-level adaptability with minimal computational overhead.

2.2. Low-Rank Adaptation for Vision-Language Models

LoRA, proposed by Hu et al. [16] as a low-rank parameter adaptation method for efficiently fine-tuning large language models. It injects trainable low-rank matrices into the weight layers of a Transformer while freezing the original weights, significantly reducing the number of tunable parameters and memory usage without sacrificing performance. This paradigm has since been extended to computer vision tasks [28, 42, 52, 62, 64], where LoRA and similar techniques have enabled efficient fine-tuning of both convolutional and Transformer-based models.

For vision-language models such as CLIP [10], recent efforts have explored LoRA as an alternative to prompt tuning. CLIP-LoRA [57] demonstrates promising results in few-shot classification, outperforming several prompt-based approaches on task-specific benchmarks. However, their evaluation primarily focuses on tasks without domain shifts, leaving LoRA’s generalization ability largely unexplored. In contrast, our work is the first to systematically explore and evaluate the generalization potential of LoRA in vision-language fine-tuning, covering base-to-novel class generalization, image domain generalization, and cross-dataset generalization. This analysis not only complements existing studies but also provides a deeper understanding of LoRA’s strengths in few-shot VLM adaptation.

2.3. Regularization Strategies

Regularization plays a critical role in improving model generalization, particularly in few-shot learning. Traditional regularization techniques can be broadly categorized into two families. The first includes constraint-based methods such as weight decay [30, 59] and adversarial training [11], which impose restrictions on model capacity or parameter updates to prevent overfitting. The second family comprises input- or parameter-dependent strategies, such as data augmentation [3, 22, 38, 47, 48, 56, 60], dropout [45], ensembling [18, 53], and label smoothing [36, 46]. These methods improve model robustness and performance in unseen scenarios by increasing diversity at the input level.

While effective, most existing techniques regularize either the input space or the optimization target. In contrast, our work introduces a gradient-based regularization method that directly steers the optimization trajectory. Specifically, we draw inspiration from Sharpness-Aware Minimization (SAM) [9], which updates parameters based on the worst-case loss in the local neighborhood. Instead of directly adopting the perturbed gradient, we leverage the gradient computed by SAM as a correction signal to refine the original gradient. To maintain update stability, we remove components from the SAM gradient that conflict with the direction of the original gradient. This approach implicitly regularizes the training dynamics by guiding optimization toward a stable region in parameter space, corresponding to a flatter area in the loss landscape, which is empirically associated with better generalization [9, 35, 51, 69]. By integrating this regularization into the GLAD framework, we improve the model’s robustness against distribution shifts and overfitting, even under limited supervision.

3. Method

We propose **GLAD** (Generalizable LoRA tuning with Regularized Gradient), a fine-tuning framework designed to address the limitations of existing fine-tuning methods in few-shot settings, where limited supervision often leads to overfitting and poor generalization to unseen domains. Our method consists of three main components: (1) *LoRA-based internal adaptation baseline* (Sec.3.2), which injects low-rank modules into each Transformer layer to enable parameter-efficient tuning; (2) *visual-textual alignment via AlignNet* (Sec.3.3), which refines textual embeddings based on visual context to improve alignment; and (3) *gradient-regularized optimization method* (Sec.3.4), which stabilizes training by guiding optimization toward flatter regions in the loss landscape. Unlike previous prompt learning approaches that often rely on handcrafted model structures or complex regularization targets, GLAD enables direct representation adaptation with a simple yet effective design. An overview of the GLAD framework is illustrated in Figure 2.

3.1. Preliminaries

Sharpness-Aware Minimization (SAM) [9] is a widely adopted optimization framework designed to improve the generalization capability of neural networks. Unlike standard empirical risk minimization, which seeks a parameter set θ that minimizes the loss $\mathcal{L}(\theta)$ on training data, SAM explicitly promotes a stable region in the parameter space where small perturbations ϵ to θ result in minimal change in the loss. This corresponds to regions in the loss landscape that are relatively flat, and implies that the model is more robust to parameter perturbations and less sensitive to noise or input distributional shifts. By introducing adversarial perturbations to the model parameters during training and optimizing for performance under these perturbations,

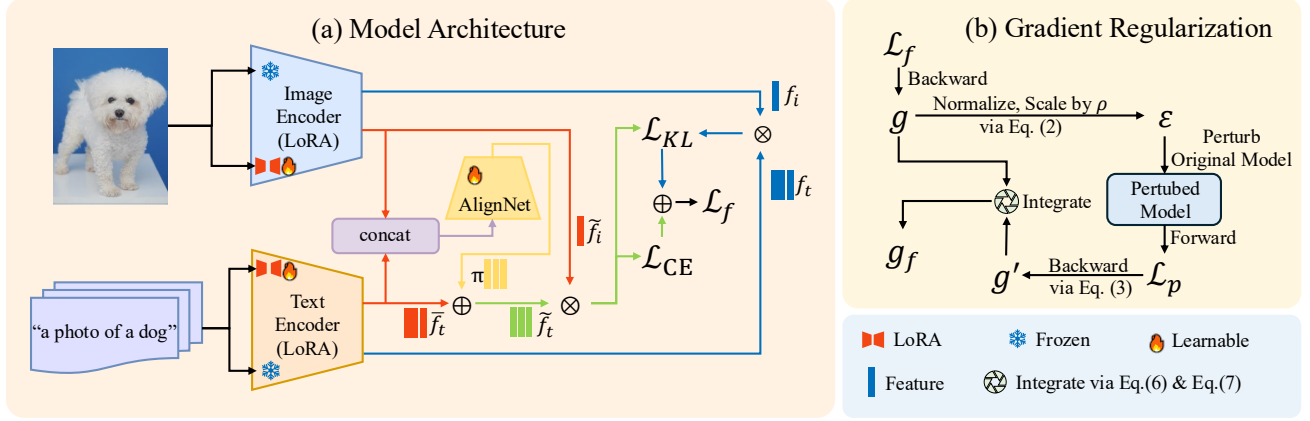


Figure 2. Overview of the GLAD framework. (a) LoRA modules are inserted into each Transformer layer of CLIP’s encoders to enable efficient adaptation. A lightweight AlignNet adjusts text features using paired image features to enhance alignment. The blue features indicate outputs from the original CLIP model, the red features represent outputs after LoRA fine-tuning, and the green lines denote features adjusted by AlignNet. During training, we apply the cross-entropy loss \mathcal{L}_{CE} for classification and the KL divergence loss \mathcal{L}_{KL} between the predicted distributions of the original and fine-tuned models to preserve zero-shot CLIP behavior. (b) To improve generalization, a gradient regularization strategy fuses gradients from the original and perturbed models, guiding optimization toward a stable region.

SAM encourages convergence to such stable regions.

Formally, SAM formulates training as a min-max optimization problem:

$$\min_{\theta} \max_{\|\epsilon\|_2 \leq \rho} \mathcal{L}(\theta + \epsilon), \quad (1)$$

where ϵ denotes an adversarial perturbation constrained within an ℓ_2 -norm ball of radius ρ , and \mathcal{L} is the training loss function. This objective encourages the model to perform well not only at the current parameter point but also in its neighborhood, leading to solutions with improved robustness and better generalization.

To solve Eq. (1) efficiently, SAM approximates the inner maximization via a first-order expansion and computes the perturbation direction as:

$$\epsilon = \rho \cdot \frac{\nabla_{\theta} \mathcal{L}(\theta)}{\|\nabla_{\theta} \mathcal{L}(\theta)\|_2}, \quad (2)$$

followed by computing the updated gradient at the perturbed parameters:

$$\nabla_{\text{SAM}} \mathcal{L}(\theta) = \nabla_{\theta} \mathcal{L}(\theta + \epsilon). \quad (3)$$

The resulting gradient reflects the worst-case local behavior.

SAM has demonstrated remarkable performance in standard supervised learning. Its ability to improve robustness against perturbations motivates our use of gradient-based regularization in few-shot learning scenarios. In Section 3.4, we present a gradient-based regularization method that uses SAM gradients to guide the optimization direction, improving performance in few-shot settings while enhancing the model’s stability to input distribution shifts and its overall generalization ability.

3.2. Internal Representation Tuning via LoRA

GLAD leverages Low-Rank Adaptation (LoRA) modules to enable efficient tuning of internal representations in both the image and text encoders of CLIP, targeting key linear projections such as the query, key, and value matrices in self-attention. This hierarchical integration enables layer-wise adaptation of intermediate features, facilitating a deeper and more distributed shift in representations toward downstream tasks.

For an input x , a hidden state h , and a weight matrix $\mathbf{W} \in \mathbb{R}^{M \times N}$, each LoRA module introduces a low-rank residual $\Delta \mathbf{W} = \mathbf{B}\mathbf{A}$, where $\mathbf{A} \in \mathbb{R}^{r \times N}$ and $\mathbf{B} \in \mathbb{R}^{M \times r}$ with rank $r \ll \min(M, N)$. The output is computed as:

$$h = \mathbf{W}x + \gamma \Delta \mathbf{W}x = \mathbf{W}x + \gamma \mathbf{B}(\mathbf{A}x), \quad (4)$$

where γ is a scaling factor, \mathbf{W} is frozen during training, and only the low-rank matrices \mathbf{A} and \mathbf{B} are updated.

This enables GLAD to efficiently adapt to new tasks by introducing only about 1% additional parameters, without forgetting the knowledge stored in the pretrained weights. As shown in Table 4, this design preserves the advantages of parameter efficiency while significantly improving downstream task adaptability and maintaining robustness to input distribution shifts. An illustration of this architecture is shown in Figure 2(a). Additionally, unlike prompt learning, which introduces extra input tokens, the LoRA modules can be merged into the original weight matrices ($\mathbf{W}_{\text{merged}} = \mathbf{W} + \gamma \Delta \mathbf{W}$) during inference, improving inference efficiency.

Algorithm 1 Gradient Regularization Algorithm

Require: Model parameters θ , loss \mathcal{L} , perturbation radius ρ , mixing factor $\alpha \in [0, 1]$, small constant δ

Ensure: Regularized gradient \mathbf{g}_f

- 1: Compute original gradient: $\mathbf{g} \leftarrow \nabla_{\theta} \mathcal{L}(\theta)$
 - 2: Compute perturbation ϵ using Eq. (2)
 - 3: Compute perturbed gradient: $\mathbf{g}' \leftarrow \nabla_{\theta} \mathcal{L}(\theta + \epsilon)$ (Eq. 3)
 - 4: **if** $\langle \mathbf{g}, \mathbf{g}' \rangle < 0$ **then**
 - 5: $\mathbf{g}' \leftarrow$ projection of \mathbf{g}' onto subspace orthogonal to \mathbf{g} (Eq. 6)
 - 6: **end if**
 - 7: Interpolate: $\mathbf{g}_f \leftarrow (1 - \alpha)\mathbf{g} + \alpha\mathbf{g}'$ (Eq. 7)
 - 8: **return** \mathbf{g}_f
-

3.3. Image-Aware Text Feature Adjustment via AlignNet

In the dual-encoder architecture of CLIP, images and texts are encoded independently through separate encoders. While this design allows for efficient inference—since text embeddings can be precomputed and reused—it also limits the model’s flexibility in adapting to specific downstream tasks, where static textual representations may fail to align accurately with dynamic visual features.

To enhance task adaptability while maintaining computational efficiency, we propose a novel AlignNet module that performs post-encoding text adjustment based on static textual and dynamic visual features. The workflow of AlignNet is illustrated in Figure 2(a). Specifically, given a dynamic image feature $\tilde{\mathbf{f}}_i \in \mathbb{R}^{512}$ and a static text feature $\tilde{\mathbf{f}}_t \in \mathbb{R}^{512}$, we concatenate them to form a joint representation $[\tilde{\mathbf{f}}_i; \tilde{\mathbf{f}}_t] \in \mathbb{R}^{1024}$, which is passed through a lightweight AlignNet (MLP) to generate a bias vector $\pi \in \mathbb{R}^{512}$. The adjusted text embedding is computed as:

$$\tilde{\mathbf{f}}_t = \tilde{\mathbf{f}}_t + \pi = \tilde{\mathbf{f}}_t + \text{AlignNet}([\tilde{\mathbf{f}}_i; \tilde{\mathbf{f}}_t]). \quad (5)$$

By directly operating on the final text embeddings, AlignNet not only maintains computational efficiency, since textual features do not require re-encoding at inference time, but also enhances the model’s ability to align visual and textual semantics in a more flexible and expressive manner. The empirical results in Table 4 demonstrate that this adjustment significantly improves performance in downstream tasks without compromising generalizability.

3.4. Gradient-Regularized Optimization for Flat Minima

Few-shot tuning is highly prone to overfitting due to the limited number of training samples. In such settings, models tend to memorize the training data and exhibit high sensitivity to input variations, leading to poor generalization on unseen distributions. To alleviate this issue, we propose a

gradient-regularized optimization strategy that encourages convergence toward flatter and more stable regions of the loss surface.

Recent studies have highlighted that models with sharp minima tend to exhibit degraded performance when exposed to input or domain shifts [9, 35, 51, 69]. In contrast, solutions that lie in flatter regions of the loss landscape are empirically associated with better generalization.

Since Sharpness-Aware Minimization (SAM) has demonstrated strong performance in finding flatter loss landscapes, we first explore its effectiveness in few-shot learning scenarios. As shown in Table 4, we find that while SAM helps preserve CLIP’s original generalization ability, it struggles to adapt to downstream tasks using only a small number of samples. To address this, we design a regularization strategy that leverages the perturbed gradient direction as a reference without altering the main optimization direction. Our goal is to guide the model toward flatter regions of the loss landscape while preserving the descent direction of the original gradient. The workflow of this regularization process is illustrated in Figure 2(b).

Specifically, let \mathbf{g} denote the gradient of the loss with respect to model parameters, and let \mathbf{g}' be a reference gradient. We first compute the inner product $\langle \mathbf{g}, \mathbf{g}' \rangle$. If the two gradients exhibit conflicting directions (i.e., $\langle \mathbf{g}, \mathbf{g}' \rangle < 0$), we remove the opposing component from \mathbf{g}' by projecting it onto the subspace orthogonal to \mathbf{g} :

$$\mathbf{g}' \leftarrow \mathbf{g}' - \frac{\langle \mathbf{g}, \mathbf{g}' \rangle}{\|\mathbf{g}\|^2 + \delta} \cdot \mathbf{g}, \quad \text{if } \langle \mathbf{g}, \mathbf{g}' \rangle < 0, \quad (6)$$

where δ is a small constant to ensure numerical stability.

We then compute the final update direction by linearly interpolating between the original and adjusted gradients:

$$\mathbf{g}_f = (1 - \alpha)\mathbf{g} + \alpha\mathbf{g}', \quad (7)$$

where $\alpha \in [0, 1]$ is a mixing coefficient.

This fused gradient \mathbf{g}_f combines the original gradient with a smoothed reference gradient, guiding the optimization toward flatter regions of the loss landscape. In practice, this improves robustness to input distribution shifts while preserving learning capability in few-shot scenarios. The full procedure is outlined in Algorithm 1.

4. Experiments

We conduct extensive experiments to evaluate the effectiveness and generalization ability of our proposed GLAD under three settings: base-to-novel class generalization, image domain generalization, and cross-dataset generalization, following [17, 66]. In the subsequent sections, we present quantitative results and ablation studies to analyze the contributions of each component in GLAD.

Dataset		CLIP [40]	CoOp [67]	CoCoOp [66]	ProDA [31]	RPO [24]	MaPLe [20]	PromptSRC [21]	CLIP-LoRA [57]	GLAD (Ours)	Gain (Δ)
Average on 11 datasets	Base	69.34	82.69	80.47	81.56	81.13	82.28	84.26	84.47	85.05	+0.58
	Novel	74.22	63.22	71.69	72.30	75.00	75.14	<u>76.10</u>	74.22	76.74	+2.52
	HM	71.70	71.66	75.83	76.65	77.94	78.55	<u>79.97</u>	79.01	80.68	+1.67
ImageNet	Base	72.43	76.47	75.98	75.40	76.60	76.66	77.60	<u>77.73</u>	79.03	+1.30
	Novel	68.14	67.88	70.43	70.23	71.57	70.54	70.73	69.17	<u>71.43</u>	+2.26
	HM	70.22	71.92	73.10	72.72	74.00	73.47	<u>74.01</u>	73.20	75.04	+1.84
Caltech101	Base	96.84	98.00	97.96	98.27	97.97	97.74	<u>98.10</u>	97.83	98.20	+0.37
	Novel	94.00	89.81	93.81	93.23	<u>94.37</u>	94.36	94.03	93.83	94.83	+1.00
	HM	95.40	93.73	95.84	95.68	<u>96.14</u>	96.02	96.02	95.79	96.49	+0.70
OxfordPets	Base	91.17	93.67	95.20	<u>95.43</u>	94.63	<u>95.43</u>	95.33	95.33	95.87	+0.54
	Novel	97.26	95.29	97.69	97.83	97.50	97.76	97.30	<u>97.77</u>	97.70	-0.07
	HM	94.12	94.47	96.43	96.62	96.04	<u>96.58</u>	96.30	95.53	96.78	+1.25
Stanford Cars	Base	63.37	78.12	70.49	74.70	73.87	72.94	<u>78.27</u>	81.23	81.60	+0.37
	Novel	74.89	60.40	73.59	71.20	75.53	74.00	<u>74.97</u>	71.93	74.93	+3.00
	HM	68.65	68.13	72.01	72.91	74.69	73.47	<u>76.58</u>	76.30	78.12	+1.82
Flowers102	Base	72.08	97.60	94.87	97.70	94.13	95.92	<u>98.07</u>	97.70	98.33	+0.63
	Novel	77.80	59.67	71.75	68.68	76.67	72.46	76.50	72.63	75.40	+2.77
	HM	74.83	74.06	81.71	80.66	84.51	82.56	85.95	83.32	<u>85.35</u>	+2.03
Food101	Base	90.10	88.33	<u>90.70</u>	90.30	90.33	90.71	90.67	90.07	90.90	+0.83
	Novel	91.22	82.26	91.29	88.57	90.83	92.05	91.53	91.00	<u>92.03</u>	+1.03
	HM	90.66	85.19	90.99	89.43	90.58	<u>91.38</u>	91.10	90.53	91.46	+0.93
FGVC Aircraft	Base	27.19	40.44	33.41	36.90	37.33	37.44	<u>42.73</u>	43.80	43.90	+0.10
	Novel	36.29	22.30	23.71	34.13	34.20	35.61	<u>37.87</u>	34.47	38.33	+3.86
	HM	31.09	28.75	27.74	35.46	35.70	36.50	<u>40.15</u>	38.58	40.93	+2.35
SUN397	Base	69.36	80.60	79.74	78.67	80.60	80.82	<u>82.67</u>	82.03	83.23	+1.20
	Novel	75.35	65.89	76.86	76.93	77.80	<u>78.70</u>	78.47	77.67	79.77	+2.10
	HM	72.23	72.51	78.27	77.79	79.18	<u>79.75</u>	<u>80.52</u>	79.79	81.46	+1.67
DTD	Base	53.24	79.44	77.01	80.67	76.70	80.36	<u>83.37</u>	83.00	84.43	+1.43
	Novel	59.90	41.18	56.00	56.48	62.13	59.18	<u>62.97</u>	59.33	64.03	+4.70
	HM	56.37	54.24	64.85	66.44	68.65	68.16	<u>71.75</u>	69.20	72.83	+3.63
EuroSAT	Base	56.48	92.19	87.49	83.90	86.63	<u>94.07</u>	92.90	94.30	91.83	-2.47
	Novel	64.05	54.74	60.04	66.00	68.97	73.23	<u>73.90</u>	70.63	77.77	+7.14
	HM	60.03	68.69	71.21	73.88	76.80	<u>82.35</u>	82.32	80.77	84.22	+3.45
UCF101	Base	70.53	84.69	82.33	85.23	83.67	83.00	<u>87.10</u>	86.20	88.13	+1.93
	Novel	77.50	56.05	73.45	71.97	75.43	78.66	<u>78.80</u>	78.03	80.03	+2.00
	HM	73.85	67.46	77.64	78.04	79.34	80.77	<u>82.74</u>	81.91	83.88	+1.97

Table 1. Base-to-novel generalization results on 11 datasets. ‘Base’ and ‘Novel’ indicate accuracy on base and novel classes, respectively, while ‘HM’ denotes their harmonic mean. ‘Gain’ shows the improvement of GLAD over the CLIP-LoRA baseline. Our method achieves clear gains over the baseline and demonstrates strong generalization ability, achieving the best or second best HM on all datasets. **Bold** indicates the best result, underline indicates the second best. Blue indicates improvement and red indicates decrease.

4.1. Experimental Settings

Datasets. We conduct experiments on eleven widely-used image classification benchmarks spanning a diverse range of domains and difficulty levels. These include: ImageNet [5], Caltech101 [7], Oxford-Pets [39], Stanford-Cars [23], Flowers102 [37], Food101 [1], FGVC-Aircraft [33], SUN397 [54], UCF101 [44], DTD [4], and EuroSAT [13]. These datasets cover a wide spectrum, including object recognition, fine-grained classification, scene understanding, texture analysis, and satellite imagery.

Evaluation Protocol. To comprehensively evaluate model generalization, we conduct experiments under three settings following [17, 66]: (1) base-to-novel class generalization, where the data is split into base and novel subsets by category, and models are trained on base classes with 16-shot supervision and tested on unseen novel classes; (2) image domain generalization, where models trained on Im-

ageNet are evaluated on four domain-shifted variants; and (3) cross-dataset evaluation, where ImageNet-trained models are tested on ten diverse classification benchmarks without additional fine-tuning.

Baselines. We compare GLAD with zero-shot CLIP [40] and a series of strong prompt tuning methods, including CoOp [67], CoCoOp [66], ProDA [31], RPO [24], MaPLe [20], PromptSRC [21], as well as a baseline CLIP-LoRA [57] that is trained using the original LoRA on CLIP. All of these baselines are trained under the same few-shot splits and training configurations for fair comparison.

Implementation Details. We implement LoRA with rank $r = 8$ for all inserted modules. AlignNet is designed as an MLP with hidden dimensions 256 and 128. For gradient regularization, we set regularization strength $\alpha = 0.5$ and perturbation strength $\rho = 0.1$. Training runs for 20 epochs with a cosine annealing learning rate schedule, start-

	Source		Target									
	ImageNet	Caltech101	OxfordPets	StanfordCars	Flowers102	Food101	Aircraft	SUN397	DTD	EuroSAT	UCF101	Average
CoOp	71.51	93.70	89.14	64.51	68.71	85.30	18.47	64.15	41.92	46.39	66.55	63.88
Co-CoOp	71.02	94.43	90.14	65.32	<u>71.88</u>	86.06	22.94	<u>67.36</u>	45.73	45.37	68.21	65.74
MaPLe	70.72	93.53	<u>90.49</u>	65.5	72.23	<u>86.20</u>	24.74	67.01	46.49	48.06	68.69	<u>66.30</u>
PromptSRC	71.27	93.60	<u>90.25</u>	<u>65.70</u>	70.25	86.15	23.90	67.10	46.87	45.50	68.75	65.81
CLIP-LoRA	73.00	92.50	88.13	57.77	64.67	81.90	20.03	64.30	42.07	44.30	64.50	62.02
GLAD (Ours)	<u>71.83</u>	<u>93.97</u>	90.83	66.43	72.23	86.47	23.83	68.60	47.10	<u>47.73</u>	69.27	66.65
Gain (Δ)	-1.17	+1.47	+2.70	+8.66	+7.56	+4.57	+3.80	+4.30	+5.03	+3.43	+4.77	+4.63

Table 2. Cross-dataset generalization results. All models are trained on ImageNet and directly evaluated on 11 unseen datasets without further adaptation. ‘Gain’ shows the improvement of GLAD over the LoRA baseline. Our method significantly improves cross-dataset generalization over the baseline, achieving the best or second best result on 9 out of 10 target datasets, and obtains the highest overall average accuracy across all target domains. **Bold** indicates the best result, underline indicates the second best result, blue indicates improvement, and red indicates decrease compared to the baseline CLIP-LoRA.

ing from 0.001. The CLIP backbone is frozen to retain pre-trained knowledge. All experiments use a single NVIDIA RTX 3090 GPU (24GB memory). Results are averaged over three random seeds for robustness and reproducibility.

	Source	Target				
	ImageNet	-V2	-S	-A	-R	Avg.
CLIP	66.73	60.83	46.15	47.77	73.96	57.18
CoOp	71.51	64.20	47.99	49.71	75.21	59.28
Co-CoOp	71.02	64.07	48.75	50.63	76.18	59.91
MaPLe	70.72	64.07	49.15	<u>50.90</u>	76.98	60.27
PromptSRC	71.27	64.35	<u>49.55</u>	<u>50.90</u>	77.80	<u>60.65</u>
CLIP-LoRA	73.00	65.17	45.97	44.17	72.67	57.00
GLAD (Ours)	<u>71.83</u>	<u>64.93</u>	49.80	51.03	<u>77.43</u>	60.80
Gain (Δ)	-1.17	-0.24	+3.83	+6.86	+4.76	+3.80

Table 3. Domain generalization results. All methods are trained on ImageNet and evaluated on four out-of-distribution variants: ImageNet-V2, -Sketch, -A, and -R. ‘Gain’ shows the improvement of GLAD over the CLIP-LoRA baseline. GLAD achieves a substantial lead in target domain average accuracy and shows strong robustness to distribution shifts. **Bold** indicates the best result, underline indicates the second best, blue indicates improvement and red indicates decrease compared to the baseline.

4.2. Main Results

Base-to-Novel Generalization. We evaluate GLAD on the base-to-novel class generalization task, where each dataset is split into disjoint base and novel categories, and models are trained with 16-shot supervision on base classes. We compare against zero-shot CLIP [40], CLIP-LoRA baseline, and several prompt-based methods, including CoOp [67], CoCoOp [66], ProDA [31], RPO [24], MaPLe [20], and PromptSRC [21]. Results on 11 benchmarks are shown in Table 1.

GLAD achieves the highest average accuracy on both base (85.05%) and novel (76.74%) classes, significantly im-

proving over the LoRA baseline (+1.67% HM gain) and surpassing prior methods. It attains the best average HM of 80.68%, outperforming the strongest baseline PromptSRC by 0.71% in HM, demonstrating balanced generalization across seen and unseen classes.

Across datasets, GLAD ranks first in HM on 7 out of 11 datasets and second on the rest, showing strong performance not only on large benchmarks like ImageNet and Caltech101, but also on challenging domains such as FGVC Aircraft, DTD, and SUN397. These results highlight GLAD’s clear advantage in base-to-novel generalization and its state-of-the-art accuracy across diverse tasks.

Domain Generalization. To evaluate GLAD’s robustness under distribution shifts, we follow standard domain generalization protocol: all models are trained on ImageNet [5] and directly tested on four out-of-distribution (OOD) variants: ImageNet-V2 [41], ImageNet-Sketch [50], ImageNet-A [15], and ImageNet-R [14] without additional fine-tuning. These target datasets introduce diverse domain shifts, such as low-level distortions (Sketch), adversarial filtering (A), and artistic style variations (R).

As shown in Table 3, GLAD achieves clear improvements over the CLIP-LoRA baseline on target domains, boosting average target accuracy by +3.80%. Notably, GLAD achieves the best accuracy on ImageNet-Sketch (49.80%), ImageNet-A (51.03%), and the highest overall target average (60.80%), outperforming prior prompt-based methods including MaPLe (60.27%) and PromptSRC (60.65%). It also secures competitive performance on ImageNet-R (77.43%) and ImageNet-V2 (64.93%).

These results demonstrate that GLAD not only enhances performance over CLIP-LoRA [57] under domain shifts but also provides robust and generalizable vision-language adaptation compared to existing prompt tuning methods.

	LoRA	SAM	GradReg	AlignNet	Base	Novel	H
(a)	✓				84.47	74.22	79.01
(b)	✓	✓			83.79	76.54	80.00
(c)	✓		✓		84.60	76.57	80.38
(d)	✓			✓	84.82	74.76	79.81
(e)	✓		✓	✓	85.05	76.74	80.68

Table 4. Ablation study on individual GLAD components. We report average performance over 11 datasets. LoRA denotes low-rank adaptation for internal representation tuning and serves as the baseline. GradReg refers to the gradient regularization strategy. AlignNet adjusts static text embeddings conditioned on dynamic visual features. Compared to the LoRA baseline, SAM improves novel accuracy but slightly reduces base accuracy. Gradient Regularization retains SAM’s benefits for novel classes while preserving base performance. AlignNet enhances both base and novel accuracy, and combining AlignNet with GradReg achieves the best overall performance. ‘Base’, ‘Novel’, and ‘H’ refer to accuracy on base classes, novel classes, and their harmonic mean, respectively.

Cross-Dataset Generalization. We evaluate GLAD’s transferability by training on ImageNet [5] and directly testing on ten out-of-distribution (OOD) datasets without further adaptation. These datasets cover diverse domains, including objects, scenes, textures, fine-grained categories, and actions, offering a comprehensive test of cross-dataset generalization.

As shown in Table 2, GLAD achieves substantial improvements over the CLIP-LoRA baseline, boosting average accuracy across target domains by +4.63%. It achieves the best or second-best accuracy on 9 out of 10 target datasets, demonstrating robust generalization across various domains. Notably, GLAD delivers large gains on challenging datasets like StanfordCars (+8.66%), Flowers102 (+7.56%), and DTD (+5.03%). Compared to existing prompt-based methods, GLAD consistently achieves higher accuracy, including the highest average target accuracy (66.65%), surpassing MaPLe (66.30%) and PromptSRC (65.81%).

These results highlight that GLAD provides significant advantages over LoRA and prior prompt tuning methods, offering a strong and reliable solution for cross-domain transfer in vision-language models.

4.3. Ablation Studies

To better understand the contribution of each GLAD component, we conduct ablation studies, with results shown in Table 4. We analyze the individual and combined effects of SAM, Gradient Regularization, and AlignNet, and provide detailed insights into their impact.

Effectiveness of SAM. As shown in row (b), adding SAM to the LoRA baseline improves novel accuracy from 74.22% to 76.54%, confirming that SAM helps the model find flatter minima that generalize better to unseen categories. However, this comes at the cost of a slight drop

in base accuracy (from 84.47% to 83.79%). This suggests that although SAM enhances generalization, its optimization landscape may limit the model’s ability to fully exploit the training data in low-shot settings, making convergence to low-loss regions on base classes more difficult.

Effectiveness of Gradient Regularization. In row (c), replacing SAM with Gradient Regularization raises novel accuracy further to 76.57% while recovering base accuracy to 84.60%. This shows that Gradient Regularization inherits SAM’s generalization advantage without sacrificing learning capacity. The strategy promotes smoother solutions that generalize well, while still allowing the model to effectively fit the training data on base classes.

Effectiveness of AlignNet. Row (d) demonstrates that adding AlignNet to LoRA improves both base and novel accuracy (84.82% and 74.76%, respectively). AlignNet introduces dynamic adjustments to static text embeddings based on visual inputs, providing additional flexibility that allows the model to better align vision and language features. This helps the model adapt more effectively to both seen and unseen categories, leading to balanced performance.

Synergy of All Components. Finally, the full GLAD model (row e), which combines LoRA, Gradient Regularization, and AlignNet, achieves the best overall performance: 85.05% base accuracy, 76.74% novel accuracy, and 80.68% harmonic mean. This indicates that the components complement each other: Gradient Regularization ensures generalization without harming learning ability, while AlignNet further enhances flexibility and alignment between modalities. Their combination enables GLAD to achieve robust and balanced performance across base and novel classes in few-shot scenarios.

These findings highlight that each component plays a distinct role: SAM and Gradient Regularization primarily improve generalization, AlignNet provides adaptability, and together they create a stronger model that balances learning and generalization under challenging conditions.

5. Conclusion

We present GLAD, a parameter-efficient fine-tuning framework designed to enhance the generalization of vision-language models. GLAD integrates three key components: a low-rank adaptation baseline, a lightweight multi-modal fusion module, and a gradient-based regularization strategy. By updating only a small set of parameters while keeping the CLIP backbone frozen, GLAD achieves robust performance under distribution shifts and consistently outperforms existing prompt tuning approaches in few-shot scenarios. Our ablation analysis examines each component’s contribution and shows how Gradient Regularization overcomes the limitations of SAM in low-shot settings. Overall, GLAD offers an effective, efficient solution for adapting vision-language models with limited supervision while ensuring strong generalization across tasks.

References

- [1] Lukas Bossard, Matthieu Guillaumin, and Luc Van Gool. Food-101—mining discriminative components with random forests. In *ECCV*, pages 446–461. Springer, 2014. 6
- [2] Qinglong Cao, Zhengqin Xu, Yuntian Chen, Chao Ma, and Xiaokang Yang. Domain prompt learning with quaternion networks. In *Proceedings of the IEEE/CVF Conference on Computer Vision and Pattern Recognition*, pages 26637–26646, 2024. 3
- [3] Hyeon Kyu Choi, Joonmyung Choi, and Hyunwoo J Kim. Tokenmixup: Efficient attention-guided token-level data augmentation for transformers. In *NeurIPS*, 2023. 3
- [4] Mircea Cimpoi, Subhransu Maji, Iasonas Kokkinos, Sammy Mohamed, and Andrea Vedaldi. Describing textures in the wild. In *CVPR*, pages 3606–3613, 2014. 6
- [5] Jia Deng, Wei Dong, Richard Socher, Li-Jia Li, Kai Li, and Li Fei-Fei. Imagenet: A large-scale hierarchical image database. In *CVPR*, pages 248–255. Ieee, 2009. 6, 7, 8
- [6] Yu Du, Fangyun Wei, Ziheng Zhang, Miaoqing Shi, Yue Gao, and Guoqi Li. Learning to prompt for open-vocabulary object detection with vision-language model. In *CVPR*, 2022. 1
- [7] Li Fei-Fei, Rob Fergus, and Pietro Perona. Learning generative visual models from few training examples: An incremental bayesian approach tested on 101 object categories. In *CVPR Workshop*, pages 178–178. IEEE, 2004. 6
- [8] Chengjian Feng, Yujie Zhong, Zequn Jie, Xiangxiang Chu, Haibing Ren, Xiaolin Wei, Weidi Xie, and Lin Ma. Promptdet: Towards open-vocabulary detection using uncured images. In *ECCV*, 2022. 1
- [9] Pierre Foret, Ariel Kleiner, Hossein Mobahi, and Behnam Neyshabur. Sharpness-aware minimization for efficiently improving generalization. *arXiv preprint arXiv:2010.01412*, 2020. 3, 5
- [10] Peng Gao, Shijie Geng, Renrui Zhang, Teli Ma, Rongyao Fang, Yongfeng Zhang, Hongsheng Li, and Yu Qiao. Clip-adapter: Better vision-language models with feature adapters. *arXiv preprint arXiv:2110.04544*, 2021. 3
- [11] Ian J Goodfellow, Jonathon Shlens, and Christian Szegedy. Explaining and harnessing adversarial examples. *arXiv preprint arXiv:1412.6572*, 2014. 3
- [12] Xiuye Gu, Tsung-Yi Lin, Weicheng Kuo, and Yin Cui. Open-vocabulary object detection via vision and language knowledge distillation. In *ICLR*, 2022. 1
- [13] Patrick Helber, Benjamin Bischke, Andreas Dengel, and Damian Borth. Eurosat: A novel dataset and deep learning benchmark for land use and land cover classification. *J-STARS*, 12(7):2217–2226, 2019. 6
- [14] Dan Hendrycks, Steven Basart, Norman Mu, Saurav Kadavath, Frank Wang, Evan Dorundo, Rahul Desai, Tyler Zhu, Samyak Parajuli, Mike Guo, et al. The many faces of robustness: A critical analysis of out-of-distribution generalization. In *ICCV*, pages 8340–8349, 2021. 7
- [15] Dan Hendrycks, Kevin Zhao, Steven Basart, Jacob Steinhardt, and Dawn Song. Natural adversarial examples. In *CVPR*, pages 15262–15271, 2021. 7
- [16] Edward J Hu, Yelong Shen, Phillip Wallis, Zeyuan Allen-Zhu, Yuanzhi Li, Shean Wang, Lu Wang, Weizhu Chen, et al. Lora: Low-rank adaptation of large language models. *ICLR*, 1(2):3, 2022. 1, 3
- [17] Yukun Huang, Kun Qian, and Zhou Yu. Learning a better initialization for soft prompts via meta-learning. *arXiv preprint arXiv:2205.12471*, 2022. 5, 6
- [18] Gabriel Ilharco, Mitchell Wortsman, Samir Yitzhak Gadre, Shuran Song, Hannaneh Hajishirzi, Simon Kornblith, Ali Farhadi, and Ludwig Schmidt. Patching open-vocabulary models by interpolating weights. *arXiv preprint arXiv:2208.05592*, 2022. 3
- [19] Menglin Jia, Luming Tang, Bor-Chun Chen, Claire Cardie, Serge Belongie, Bharath Hariharan, and Ser-Nam Lim. Visual prompt tuning. In *ECCV*, 2022. 3
- [20] Muhammad Uzair Khattak, Hanoona Rasheed, Muhammad Maaz, Salman Khan, and Fahad Shahbaz Khan. Maple: Multi-modal prompt learning. In *CVPR*, pages 19113–19122, 2023. 1, 3, 6, 7
- [21] Muhammad Uzair Khattak, Syed Talal Wasim, Muzammal Naseer, Salman Khan, Ming-Hsuan Yang, and Fahad Shahbaz Khan. Self-regulating prompts: Foundational model adaptation without forgetting. In *Proceedings of the IEEE/CVF international conference on computer vision*, pages 15190–15200, 2023. 1, 3, 6, 7
- [22] Jang-Hyun Kim, Wonho Choo, Hosan Jeong, and Hyun Oh Song. Co-mixup: Saliency guided joint mixup with super-modular diversity. In *ICLR*, 2021. 3
- [23] Jonathan Krause, Michael Stark, Jia Deng, and Li Fei-Fei. 3d object representations for fine-grained categorization. In *ICCV*, pages 554–561, 2013. 6
- [24] Dongjun Lee, Seokwon Song, Jihee Suh, Joonmyeong Choi, Sanghyeok Lee, and Hyunwoo J Kim. Read-only prompt optimization for vision-language few-shot learning. In *ICCV*, 2023. 1, 3, 6, 7
- [25] Brian Lester, Rami Al-Rfou, and Noah Constant. The power of scale for parameter-efficient prompt tuning. In *EMNLP*, 2021. 2
- [26] Junnan Li, Dongxu Li, Silvio Savarese, and Steven Hoi. Blip-2: Bootstrapping language-image pre-training with frozen image encoders and large language models. In *ICML*, 2023. 1
- [27] Zheng Li, Xiang Li, Xinyi Fu, Xin Zhang, Weiqiang Wang, Shuo Chen, and Jian Yang. Promptkd: Unsupervised prompt distillation for vision-language models. In *Proceedings of the IEEE/CVF Conference on Computer Vision and Pattern Recognition*, pages 26617–26626, 2024. 3
- [28] Haotian Liu, Chunyuan Li, Qingyang Wu, and Yong Jae Lee. Visual instruction tuning. *Advances in neural information processing systems*, 36:34892–34916, 2023. 3
- [29] Pengfei Liu, Weizhe Yuan, Jinlan Fu, Zhengbao Jiang, Hiroaki Hayashi, and Graham Neubig. Pre-train, prompt, and predict: A systematic survey of prompting methods in natural language processing. *ACM computing surveys*, 55(9): 1–35, 2023. 2
- [30] Ilya Loshchilov and Frank Hutter. Decoupled weight decay regularization. In *ICLR*, 2019. 3

- [31] Yuning Lu, Jianzhuang Liu, Yonggang Zhang, Yajing Liu, and Xinmei Tian. Prompt distribution learning. In *CVPR*, pages 5206–5215, 2022. 1, 6, 7
- [32] Timo Lüddecke and Alexander Ecker. Image segmentation using text and image prompts. In *CVPR*, pages 7086–7096, 2022. 1
- [33] Subhransu Maji, Esa Rahtu, Juho Kannala, Matthew Blaschko, and Andrea Vedaldi. Fine-grained visual classification of aircraft. *arXiv preprint arXiv:1306.5151*, 2013. 6
- [34] Ron Mokady, Amir Hertz, and Amit H Bermano. Clipcap: Clip prefix for image captioning. *arXiv:2111.09734*, 2021. 1
- [35] Gonalo Mordido, Pranshu Malviya, Aristide Baratin, and Sarath Chandar. Lookbehind-sam: k steps back, 1 step forward. *arXiv preprint arXiv:2307.16704*, 2023. 3, 5
- [36] Rafael Mller, Simon Kornblith, and Geoffrey E Hinton. When does label smoothing help? *Advances in neural information processing systems*, 32, 2019. 3
- [37] Maria-Elena Nilsback and Andrew Zisserman. Automated flower classification over a large number of classes. In *ICVGIP*, pages 722–729. IEEE, 2008. 6
- [38] Hyeonjin Park, Seunghun Lee, Sihyeon Kim, Jinyoung Park, Jisu Jeong, Kyung-Min Kim, Jung-Woo Ha, and Hyunwoo J Kim. Metropolis-hastings data augmentation for graph neural networks. In *NeurIPS*, 2022. 3
- [39] Omkar M Parkhi, Andrea Vedaldi, Andrew Zisserman, and CV Jawahar. Cats and dogs. In *CVPR*, pages 3498–3505. IEEE, 2012. 6
- [40] Alec Radford, Jong Wook Kim, Chris Hallacy, Aditya Ramesh, Gabriel Goh, Sandhini Agarwal, Girish Sastry, Amanda Askell, Pamela Mishkin, Jack Clark, et al. Learning transferable visual models from natural language supervision. In *ICML*, 2021. 1, 6, 7
- [41] Benjamin Recht, Rebecca Roelofs, Ludwig Schmidt, and Vaishaal Shankar. Do imagenet classifiers generalize to imagenet? In *ICML*, pages 5389–5400. PMLR, 2019. 7
- [42] Ying Shen, Zhiyang Xu, Qifan Wang, Yu Cheng, Wenpeng Yin, and Lifu Huang. Multimodal instruction tuning with conditional mixture of lora. *arXiv preprint arXiv:2402.15896*, 2024. 3
- [43] Amanpreet Singh, Ronghang Hu, Vedanuj Goswami, Guillaume Couairon, Wojciech Galuba, Marcus Rohrbach, and Douwe Kiela. Flava: A foundational language and vision alignment model. In *CVPR*, 2022. 1
- [44] Khurram Soomro, Amir Roshan Zamir, and Mubarak Shah. Ucf101: A dataset of 101 human actions classes from videos in the wild. *arXiv preprint arXiv:1212.0402*, 2012. 6
- [45] Nitish Srivastava, Geoffrey Hinton, Alex Krizhevsky, Ilya Sutskever, and Ruslan Salakhutdinov. Dropout: a simple way to prevent neural networks from overfitting. *JMLR*, 15 (1):1929–1958, 2014. 3
- [46] Christian Szegedy, Vincent Vanhoucke, Sergey Ioffe, Jon Shlens, and Zbigniew Wojna. Rethinking the inception architecture for computer vision. In *CVPR*, pages 2818–2826, 2016. 3
- [47] AFM Uddin, Mst Monira, Wheemyung Shin, TaeChoong Chung, Sung-Ho Bae, et al. Saliencymix: A saliency guided data augmentation strategy for better regularization. In *ICLR*, 2021. 3
- [48] Vikas Verma, Alex Lamb, Christopher Beckham, Amir Najafi, Aaron Courville, Ioannis Mitliagkas, and Yoshua Bengio. Manifold mixup: learning better representations by interpolating hidden states. In *ICML*, 2019. 3
- [49] Dongsheng Wang, Miaoge Li, Xinyang Liu, MingSheng Xu, Bo Chen, and Hanwang Zhang. Tuning multi-mode token-level prompt alignment across modalities. *Advances in Neural Information Processing Systems*, 36:52792–52810, 2023. 3
- [50] Haohan Wang, Songwei Ge, Zachary Lipton, and Eric P Xing. Learning robust global representations by penalizing local predictive power. In *NeurIPS*, 2019. 7
- [51] Pengfei Wang, Zhaoxiang Zhang, Zhen Lei, and Lei Zhang. Sharpness-aware gradient matching for domain generalization. In *Proceedings of the IEEE/CVF Conference on Computer Vision and Pattern Recognition*, pages 3769–3778, 2023. 3, 5
- [52] Weihan Wang, Qingsong Lv, Wenmeng Yu, Wenyi Hong, Ji Qi, Yan Wang, Junhui Ji, Zhuoyi Yang, Lei Zhao, Song XiXuan, et al. Cogvlm: Visual expert for pretrained language models. *Advances in Neural Information Processing Systems*, 37:121475–121499, 2024. 3
- [53] Mitchell Wortsman, Gabriel Ilharco, Jong Wook Kim, Mike Li, Simon Kornblith, Rebecca Roelofs, Raphael Gontijo Lopes, Hannaneh Hajishirzi, Ali Farhadi, Hongseok Namkoong, et al. Robust fine-tuning of zero-shot models. In *CVPR*, pages 7959–7971, 2022. 3
- [54] Jianxiong Xiao, James Hays, Krista A Ehinger, Aude Oliva, and Antonio Torralba. Sun database: Large-scale scene recognition from abbey to zoo. In *CVPR*, pages 3485–3492. IEEE, 2010. 6
- [55] Hantao Yao, Rui Zhang, and Changsheng Xu. Tcpl: Textual-based class-aware prompt tuning for visual-language model. In *Proceedings of the IEEE/CVF Conference on Computer Vision and Pattern Recognition*, pages 23438–23448, 2024. 1, 3
- [56] Sangdoo Yun, Dongyoon Han, Seong Joon Oh, Sanghyuk Chun, Junsuk Choe, and Youngjoon Yoo. Cutmix: Regularization strategy to train strong classifiers with localizable features. In *CVPR*, pages 6023–6032, 2019. 3
- [57] Maxime Zanella and Ismail Ben Ayed. Low-rank few-shot adaptation of vision-language models. In *Proceedings of the IEEE/CVF Conference on Computer Vision and Pattern Recognition*, pages 1593–1603, 2024. 3, 6, 7
- [58] Xiaohua Zhai, Xiao Wang, Basil Mustafa, Andreas Steiner, Daniel Keysers, Alexander Kolesnikov, and Lucas Beyer. Lit: Zero-shot transfer with locked-image text tuning. In *CVPR*, pages 18123–18133, 2022. 1
- [59] Guodong Zhang, Chaoqi Wang, Bowen Xu, and Roger Grosse. Three mechanisms of weight decay regularization. In *ICLR*, 2019. 3
- [60] Hongyi Zhang, Moustapha Cisse, Yann N Dauphin, and David Lopez-Paz. mixup: Beyond empirical risk minimization. *arXiv preprint arXiv:1710.09412*, 2017. 3

- [61] Ji Zhang, Shihan Wu, Lianli Gao, Heng Tao Shen, and Jingkuan Song. Dept: Decoupled prompt tuning. In *Proceedings of the IEEE/CVF Conference on Computer Vision and Pattern Recognition*, pages 12924–12933, 2024. [1](#), [3](#)
- [62] Lvmin Zhang, Anyi Rao, and Maneesh Agrawala. Adding conditional control to text-to-image diffusion models. In *Proceedings of the IEEE/CVF international conference on computer vision*, pages 3836–3847, 2023. [3](#)
- [63] Renrui Zhang, Jiaming Han, Aojun Zhou, Xiangfei Hu, Shilin Yan, Pan Lu, Hongsheng Li, Peng Gao, and Yu Qiao. Llama-adapter: Efficient fine-tuning of language models with zero-init attention. In *ICLR*, 2024. [1](#)
- [64] Bo Zhao, Boya Wu, Muyang He, and Tiejun Huang. Svit: Scaling up visual instruction tuning. *arXiv preprint arXiv:2307.04087*, 2023. [3](#)
- [65] Yiwu Zhong, Jianwei Yang, Pengchuan Zhang, Chunyuan Li, Noel Codella, Liunian Harold Li, Luowei Zhou, Xiyang Dai, Lu Yuan, Yin Li, et al. Regionclip: Region-based language-image pretraining. In *CVPR*, 2022. [1](#)
- [66] Kaiyang Zhou, Jingkang Yang, Chen Change Loy, and Ziwei Liu. Conditional prompt learning for vision-language models. In *CVPR*, pages 16816–16825, 2022. [1](#), [3](#), [5](#), [6](#), [7](#)
- [67] Kaiyang Zhou, Jingkang Yang, Chen Change Loy, and Ziwei Liu. Learning to prompt for vision-language models. *IJCV*, 130(9):2337–2348, 2022. [1](#), [2](#), [6](#), [7](#)
- [68] Beier Zhu, Yulei Niu, Yucheng Han, Yue Wu, and Hanwang Zhang. Prompt-aligned gradient for prompt tuning. In *ICCV*, 2023. [1](#)
- [69] Juntang Zhuang, Boqing Gong, Liangzhe Yuan, Yin Cui, Hartwig Adam, Nicha Dvornek, Sekhar Tatikonda, James Duncan, and Ting Liu. Surrogate gap minimization improves sharpness-aware training. *arXiv preprint arXiv:2203.08065*, 2022. [3](#), [5](#)